HHS Public Access

Author manuscript

Conf Proc IEEE Eng Med Biol Soc. Author manuscript; available in PMC 2017 August 02.

Published in final edited form as:

Conf Proc IEEE Eng Med Biol Soc. 2015 August ; 2015: 1440–1443. doi:10.1109/EMBC.2015.7318640.

Structure of the set of feasible neural commands for complex motor tasks

FJ Valero-Cuevas[1], **BA Cohn**[1], **M Szedlák**[2], **K Fukuda**[2], and **B Gärtner**[2]

[1]Departments of Biomedical Engineering and Computer Science at the University of Southern California Viterbi School of Engineering, Los Angeles, CA 90089, USA [2]Department of Computer Science, ETH Zurich, Switzerland

Abstract

The brain must select its control strategies among an infinite set of possibilities; researchers believe that it must be solving an optimization problem. While this set of feasible solutions is infinite and lies in high dimensions, it is bounded by kinematic, neuromuscular, and anatomical constraints, within which the brain must select optimal solutions. That is, the set of feasible activations is well structured. However, to date there is no method to describe and quantify the structure of these high-dimensional solution spaces. Bounding boxes or dimensionality reduction algorithms do not capture their detailed structure. We present a novel approach based on the well-known Hit-and-Run algorithm in computational geometry to extract the structure of the feasible activations capable of producing 50% of maximal fingertip force in a specific direction. We use a realistic model of a human index finger with 7 muscles, and 4 DOFs. For a given static force vector at the endpoint, the feasible activation space is a 3D convex polytope, embedded in the 7D unit cube. It is known that explicitly computing the volume of this polytope can become too computationally complex in many instances. However, our algorithm was able to sample 1,000,000 uniform at random points from the feasible activation space. The computed distribution of activation across muscles sheds light onto the structure of these solution spaces—rather than simply exploring their maximal and minimal values. Although this paper presents a 7 dimensional case of the index finger, our methods extend to systems with at least 40 muscles. This will allow our motor control community to understand the distributions of feasible muscle activations, providing important contextual information into learning, optimization and adaptation of motor patterns in future research.

I. INTRODUCTION

Muscle redundancy is the term used to describe the underdetermined nature of neural control of musculature. The classical notion of muscle redundancy proposes that, faced with an infinite number of possible muscle activation patterns for a given task, the nervous system uses optimization to select a specific solution. Here, each of the N muscles represents a dimension of control, and a muscle activation pattern is a point in $[0,1]^N$ [18]. Thus researchers often seek to infer the optimization approach and the cost functions the nervous system likely uses to find points in activation space to produce natural behavior [2], [12], [13], [16], [4], [7].

Implicit in these optimization procedures is the notion that there exists a well structured set of feasible solutions. Thus several of us have focused on describing and understanding those high-dimensional subspaces embedded in $[0,1]^N$ [10], [11], [15], [18], [8].

For the case of muscle redundancy for submaximal and static force production with a limb, the problem is phrased as one of computational geometry: find the convex polytope of all feasible muscle activations given the mechanics of the limb and the constrains of the task [1], [18], [17], [8]. This convex polytope is called the *feasible activation set.* To date, the structure of this high-dimensional polytope is inferred by its bounding box [10], [15], [8]. But the bounding box of a convex polytope will always exclude the details of its shape. Empirical dimensionality-reduction methods have also been used to calculate basis vectors for such subspaces [3], [5], [9]. But those basis vectors only provide a description of the dimension, orientation, and aspect ratio of the polytope, but not of its boundaries or internal structure.

Here we present a novel application of the well-known Hit-and-Run algorithm [14] to describe the internal structure of these high-dimensional feasible activation sets. We apply our technique to a schematic example with three muscles to describe the method, and then use a realistic model of an index finger with seven muscles and four joints [18].

II. METHODS

A. Hit-and-Run algorithm

The boundaries of the convex polytope defining the feasible activation set are defined by the mechanics of the limb and the constraints of the task, as is described in Subsection II-B. The goal of the Hit-and-Run algorithm is to uniformly sample a convex body [14]. In the case of a schematic tendon-driven limb with three muscles, the feasible activation space is the unit cube (as muscles can only be activated positively from 0 to a maximal normalized value of 1). As explained in [17], when task constraints are introduced to the system, the feasible activation set is further reduced; in this context, a task is a static force vector produced at the endpoint of the limb, which is represented as a set of inequality constraints. Thus if this simple limb meets all constraints, the feasible activation set of the polygon P contains all feasible activations $\mathbf{a} \in \mathbb{R}^n$ that satisfy

$$\mathbf{f}=A\mathbf{a}, \mathbf{a} \in [0,1]^n,$$

where $\mathbf{f} \in \mathbb{R}^m$ is a fixed force vector, and $A=J^{-T}RF_o \in \mathbb{R}^{m\times n}$ —where J, R, and F_o are the matrices of the Jacobian of the limb, the moment arms of the tendons, and the strengths of the muscles, respectively [18], [17]. P is bounded by the unit n-cube since all variables $a_i, i \in [n]$ are bounded by 0 and 1 from below, above respectively. Consider the following 1×3 fabricated example, where the task is a 1N unidimensional force.

$$1=\frac{10}{3}a_1 - \frac{53}{15}a_2+2a_3$$
$$a_1, a_2, a_3 \in [0,1],$$

the set of feasible activations is given by the shaded set in Figure 1.

The Hit-and-Run walk on P is defined as follows (it works analogously for any convex body).

1. Inner Point: Find a given starting point **p** of P (Figure 2a) .
2. Direction: Generate a random direction from **p** (uniformly at random over all directions) (Figure 2a).
3. Endpoints: Find the intersection points of the random direction with the edges of the polytope (Figure 2b).
4. New Point: Pick a point uniform at random along the line segment defined by the endpoints (Figure 2c).
5. Repeat from (*a*) the above steps with the new point as the starting point.

To find a starting point in

$$\mathbf{f}=A\mathbf{a}, \mathbf{a} \in [0,1]^n,$$

we only need to find a feasible activation vector. For the Hit-and-Run algorithm to mix faster, we want the starting point to be centrally located within the polytope. We use the following standard trick with slack variables ε_i.

$$\begin{aligned} & \text{maximize} && \textstyle\sum_{i=1}^{n} \varepsilon_i \\ \text{subject to} \quad & && \mathbf{f}=A\mathbf{a} \\ & && a_i \in [\varepsilon_i, 1-\varepsilon_i], \ \ \forall i \in \{1,\ldots,n\} \\ & && \varepsilon_i \geq 0, \ \ \forall i \in \{1,\ldots,n\}. \end{aligned} \quad (1)$$

The recursive nature of the algorithm means that consecutive points are autocorrelated; it's important that each point sampled from the polytope is uniform at random, so we subset points separated by a number of iterations. For convex polygons in higher dimensions (over 40 dimensional), experimental results suggest that $\mathcal{O}(n)$ steps of the Hit-and-Run algorithm are sufficient. In particular Emiris and Fisikopoulos paper suggest that $\left(10+\frac{10}{n}\right) n$ steps are enough to converge upon the uniform distribution [6]. In the index finger model we executed the Hit-and-Run algorithm 1,000,000 times, selecting only every 100th point.

B. Realistic index finger model

We used our published model in [18] to find matrix $A \in \mathbb{R}^{4\times 7}$, where $\mathbf{a} \in \mathbb{R}^7$. The seven muscles are *flexor digitorum profundus* (FDP), *flexor digitorum superficialis* (FDS), *extensor indicis proprius* (EIP), *extensor digitorum communis* (EDC), *lumbrical* (LUM), *dorsal interosseous* (DI), and *palmar interosseous* (PI). The four degrees of freedom were ad-abduction, flexion-extension at the metacar-pophalangeal joint, and flexion-extension at the proximal and distal interphalangeal joints. The force direction we simulated is in the palmar direction in the posture shown in Figure 3.

III. RESULTS

Figure 4 shows the distributions of activations resulting from the solutions computed with Hit-and-Run sampling. This is the first time (to our knowledge) that the internal structure of the feasible activation set has been visualized for a sub-maximal force.

Notice that the lower and upper bounds of the activations (i.e., the dashed lines indicating their bounding box), are unhelpful in determining the actual density distribution of feasible activations. The activation needed for the maximal force output (thick gray line) is very often not the mode of the activations at 50% of output. It's important to note that these histograms are unidimensional- they do not illustrate the between-muscle associations.

IV. DISCUSSION

Our results and methodology raise the following ideas:

- The Hit-and-Run algorithm can explore the feasible activation space for a realistic 7-muscle finger in a way that is computationally tractable.
- For some muscles, we find that the bounding box exceptionally misconstrues the internal structure of the feasible activation set.
- The Hit-and-Run algorithm is cost-agnostic in the sense that no cost function is needed to predict the distribution of muscle activation patterns. Therefore, we can provide spatial context to where 'optimal' solutions lie within the solution space; this approach can be used to explore the consequences of different cost functions.
- The distribution of muscle activations may be intricately related to strong modes which critically affect the learning of motor tasks.

With the spatial context of the feasible activation space, we can explore the statistical tendencies of a musculoskeletal system, and better define the landscape upon which optimization occurs. This application of Hit-and-Run provides a tool to generate testable hypotheses of how coordination habits may come about, how they are learned, and how difficult or easy it is to break out of them.

Acknowledgments

*This work was supported by NIH NIAMS R01AR050520 and R01AR052345 grants, and SNF Project 200021-150055-1.

References

1. Avis D, Fukuda K. A pivoting algorithm for convex hulls and vertex enumeration of arrangements and polyhedra. Discrete & Computational Geometry. 1992; 8(3):295–313.
2. Chao EY, An KN. Graphical interpretation of the solution to the redundant problem in biomechanics. Journal of Biomechanical Engineering. 1978; 100:159–67.
3. Clewley RH, Guckenheimer JM, Valero-Cuevas FJ. Estimating effective degrees of freedom in motor systems. IEEE Trans Biomed Eng. Feb.2008 55:430–442. [PubMed: 18269978]

4. Crowninshield RD, Brand RA. A physiologically based criterion of muscle force prediction in locomotion. Journal of Biomechanics. 1981; 14(11):793–801. [PubMed: 7334039]
5. d'Avella, Andrea, Bizzi, Emilio. Shared and specific muscle synergies in natural motor behaviors. Proceedings of the National Academy of Sciences of the United States of America. 2005; 102(8): 3076–3081. [PubMed: 15708969]
6. Emiris, Ioannis Z., Fisikopoulos, Vissarion. Efficient random-walk methods for approximating polytope volume. arXiv preprint arXiv. 2013; 1312.2873
7. Higginson JS, Neptune RR, Anderson FC. Simulated parallel annealing within a neighborhood for optimization of biomechanical systems. Journal of biomechanics. 2005; 38(9):1938–1942. [PubMed: 16023483]
8. Valero-Cuevas FJ, Cohn BA, Yngvason HF, Lawrence EL. Exploring the high-dimensional structure of muscle redundancy via subject-specific and generic musculoskeletal models. J Biomech. 2015 In press.
9. Krishnamoorthy, Vijaya, Goodman, Simon, Zatsiorsky, Vladimir, Latash, Mark L. Muscle synergies during shifts of the center of pressure by standing persons: identification of muscle modes. Biological cybernetics. 2003; 89(2):152–161. [PubMed: 12905043]
10. Kutch, Jason J., Valero-Cuevas, Francisco J. Muscle redundancy does not imply robustness to muscle dysfunction. Journal of biomechanics. 2011; 44(7):1264–1270. [PubMed: 21420091]
11. Kutch, Jason J., Valero-Cuevas, Francisco J. Challenges and new approaches to proving the existence of muscle synergies of neural origin. PLoS computational biology. 2012; 8(5):e1002434. [PubMed: 22570602]
12. Prilutsky BI. Muscle coordination: the discussion continues. Motor Control. 2000; 4(1):97–116. 0 1087-1640 Journal article. [PubMed: 10675817]
13. Scott, Stephen H. Optimal feedback control and the neural basis of volitional motor control. Nature Reviews Neuroscience. 2004; 5(7):532–546. [PubMed: 15208695]
14. Smith, Robert L. Efficient monte carlo procedures for generating points uniformly distributed over bounded regions. Operations Research. 1984; 32(6):1296–1308.
15. Sohn, M Hongchul, McKay, J Lucas, Ting, Lena H. Defining feasible bounds on muscle activation in a redundant biomechanical task: practical implications of redundancy. Journal of biomechanics. 2013; 46(7):1363–1368. [PubMed: 23489436]
16. Todorov, Emanuel, Jordan, Michael I. Optimal feedback control as a theory of motor coordination. Nature neuroscience. 2002; 5(11):1226–1235. [PubMed: 12404008]
17. Valero-Cuevas FJ. A mathematical approach to the mechanical capabilities of limbs and fingers. Adv Exp Med Biol. 2009; 629:619–633. [PubMed: 19227524]
18. Valero-Cuevas FJ, Zajac FE, Burgar CG. Large index-fingertip forces are produced by subject-independent patterns of muscle excitation. J Biomech. Aug.1998 31:693–703. [PubMed: 9796669]

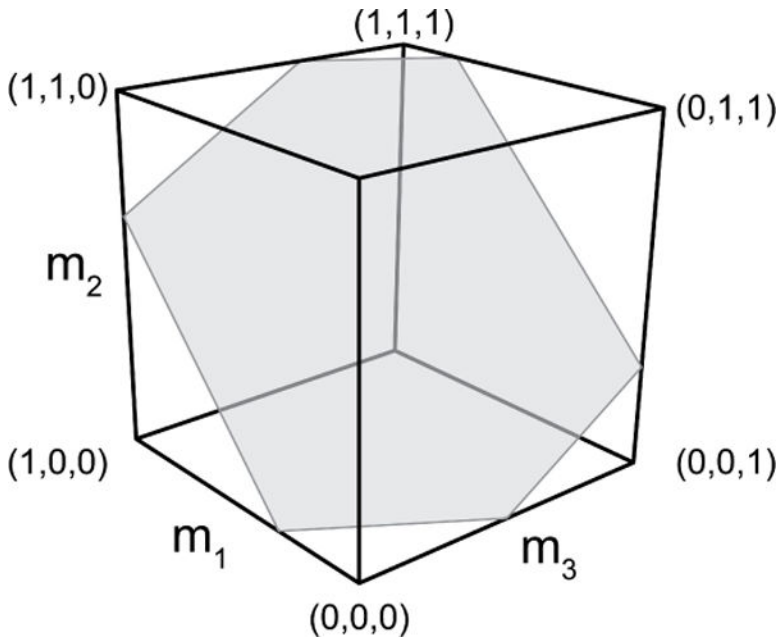

Fig. 1.

The feasible activation set for a three-muscle system meeting one functional constraint is a polygon in $\mathbb{R}^3$. Note that muscle activations are assumed to be bounded between 0 and 1.

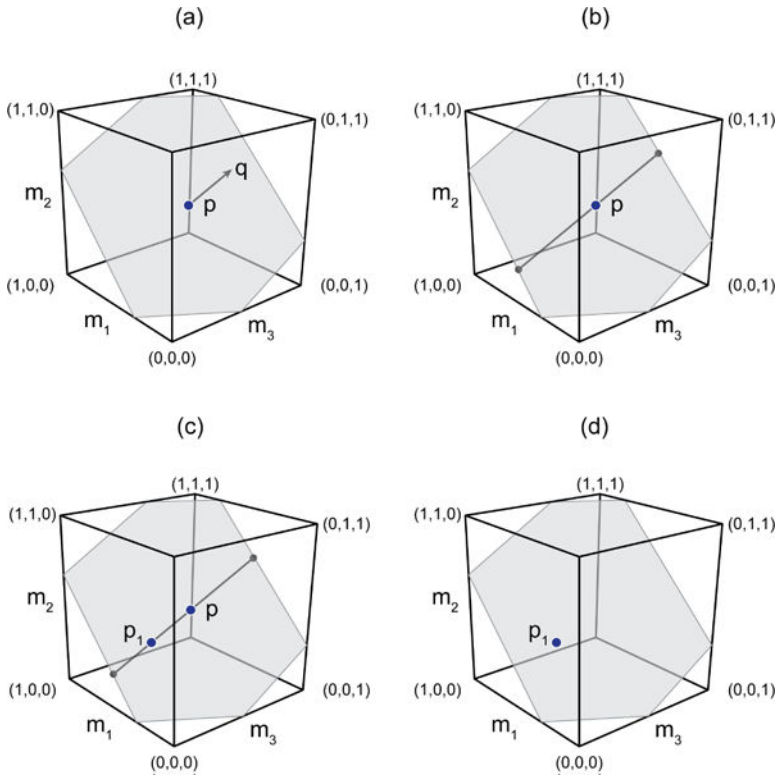

Fig. 2.
Graphical description of the Hit-and-Run algorithm.

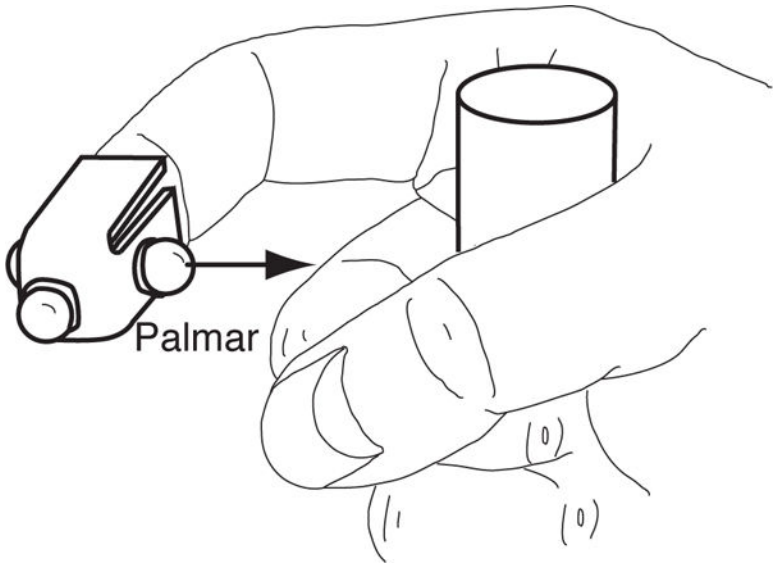

Fig. 3.
The index finger model simulated 50% of maximal force production in the palmar direction. Adapted from [18].

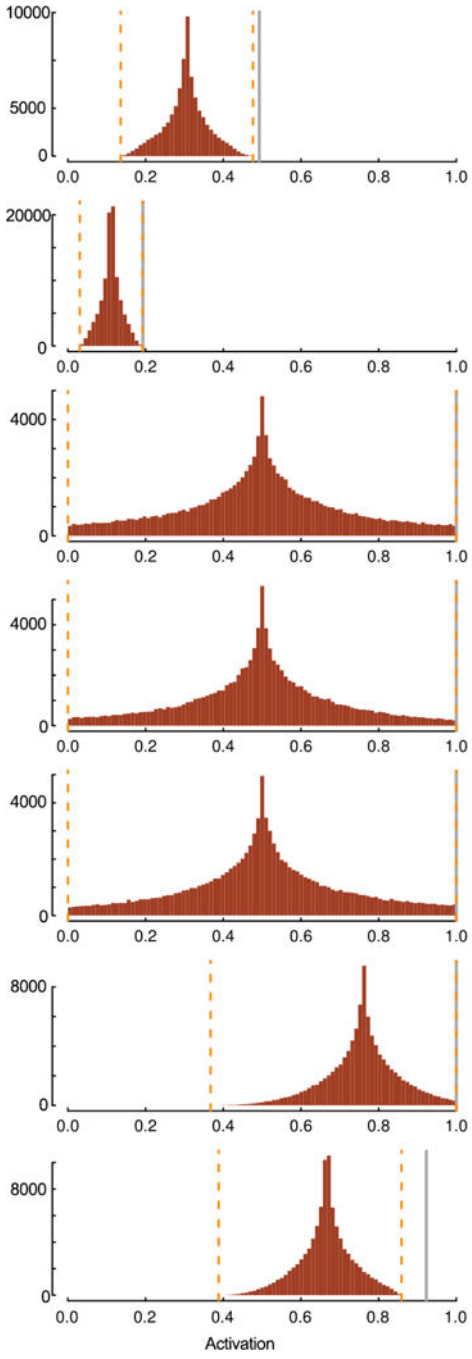

Fig. 4.

We show one histogram for each muscle of the index finger to illustrate how the muscle is used across all feasible solutions. For this set of distributions, the task was 50% of maximal force output in the palmar direction. Muscles are FDP, FDS, EIP, EDC, LUM, DI, and PI are shown in that order from top to bottom. The orange dotted lines are the lower and upper bounds of activation.